催化学报
2012 Chinese Journal of Catalysis Vol. 33 No. 8

文章编号: 0253-9837(2012)08-1347-07 国际版 DOI: 10.1016/S1872-2067(11)60422-1 研究论文: 1347~1353

Photocatalytic Synthesis of Phenol by Direct Hydroxylation of Benzene by a Modified Nanoporous Silica (LUS-1) under Sunlight

Ghasem SHIRAVAND[1], Alireza BADIEI[1,*], Ghodsi Mohammadi ZIARANI[2], Morteza JAFARABADI[1], Majid HAMZEHLOO[1]

[1]*School of Chemistry, College of Science, University of Tehran, Tehran, Iran*

[2]*Department of Chemistry, Faculty of Science, Alzahra University, Tehran, Iran*

Abstract: Fe-g-C_3N_4-LUS-1 was prepared by the thermal decomposition of dicyandiamide inside the pores of LUS-1 under an inert atmosphere. It was used as a photocatalyst for the hydroxylation of benzene to phenol in sunlight. The catalysts were characterized by Fourier transform infrared spectroscopy, N_2 adsorption-desorption, X-ray diffraction, and scanning electron microscopy. In Fe-g-C_3N_4-LUS-1, a single layer of graphitic carbon nitride (g-C_3N_4) was formed on the surface of LUS-1. The photocatalytic activity of the iron containing g-C_3N_4 based catalysts was investigated, and the catalytic activity was remarkably enhanced when the reaction condition was changed from dark to sunlight. The best result was obtained with 20%Fe-g-C_3N_4-LUS-1 in sunlight.

Key words: mesoporous silica; photocatalyst; phenol; benzene hydroxylation; sunlight; nanoporous silica; carbon nitride

CLC number: O643 **Document code:** A

Received 21 January 2012. Accepted 30 May 2012.

**Corresponding author. Tel: +98-2161112614; Fax: +98-2161113301; E-mail: abadiei@khayam.ut.ac.ir*

This work was supported by University of Tehran.

English edition available online at Elsevier ScienceDirect (http://www.sciencedirect.com/science/journal/18722067).

There is increasing interest in the photocatalytic technology in catalytic processes for hydrogen production from splitting water, self-cleaning coatings, high efficiency solar cells, and dye degradation [1–8]. These processes need considerable energy, and providing the energy is one of the most important issues. Many attempts have been made to find photocatalytic processes that utilize a renewable low cost irradiation source, such as sunlight, instead of expensive artificial irradiation sources [8–12]. Since visible light comprises a large portion of the solar energy reaching the surface of the earth, the utilization of visible light will give a more efficient solar energy usage. To achieve this, a material with a suitable band gap for absorbing visible light and that acts as an oxidative material is needed. Several materials, e.g., $Bi_{38}ZnO_{58}$ [13], CuO [14], Au/TiO_2 [15], NiO/$InTaO_4$ [16], $BiVO_4$ [17], and g-C_3N_4 [3,18], have a suitable band gap for use in photocatalytic processes under visible light irradiation and in sunlight. The band gap of graphitic carbon nitride (g-C_3N_4) was estimated to be 2.7 eV from its UV-Vis diffuse reflectance spectrum [19], which is equal to 460 nm wavelength. As a result, g-C_3N_4 can be used as a photocatalyst in the visible light region. There are several models for the structure of these compounds. The tri-s-triazine based model is the predicted most stable structure of g-C_3N_4 [20,21].

Several methods have been used to synthesize g-C_3N_4, e.g., by solid state reaction [21,22], solvothermal reaction [23,24], thermal decomposition [25], ionothermal reaction [26], and other methods [27–29]. Several precursors such as cyanamide, dicyandiamide, melamine, and cyanuric chloride have been used to get the g-C_3N_4 solid [28–31]. The easy sublimation of melamine is a serious issue in thermolysis. Dicyandiamide is recommended as a precursor to suppress this sublimation [20].

g-C_3N_4 has been used as a photocatalyst in several reactions [18,32,33]. Chen et al. [18] investigated the catalytic performance of graphitic carbon nitride for the direct hydroxylation of benzene to phenol. They reported that benzene is adsorbed and activated on g-C_3N_4, and therefore, this catalyst is a promising catalyst for the hydroxylation of benzene to phenol. In this work, graphitic carbon nitride was prepared and loaded on the surface of mesoporous Type LUS-1 silica. Due to its high surface area (800 cm^2/g), long range ordered pores (average pore diameter 3 nm) and hydrothermal stability, LUS-1 is a good support for catalytic reactions such as the hydroxylation of benzene [34]. The hydroxylation of benzene to phenol over Fe-loaded mesoporous silica, such as SBA-15 or MCM-41, with different iron contents had been investigated previously [35,36]. In this study, the properties and applications of *x*Fe-g-C_3N_4 and *x*Fe-g-C_3N_4-LUS-1 in the direct hydroxylation of benzene were studied. These reactions were carried

in just under sunlight to study if they can be used to reduce cost.

1 Experimental

1.1 Materials

Silica gel (column chromatography), sodium hydroxide, dicyandiamide, iron(III) chloride hexahydrate, acetonitrile, benzene, toluene, hydrogen peroxide (30%), and cetyltrimethylammonium bromide (Merck) and *p*-toluene-sulfonic acid monohydrate (Aldrich) of analytical grade were used without further purification.

1.2 Characterization

The catalysts were characterized by X-ray diffraction (XRD), Fourier transform infrared spectroscopy (FT-IR), scanning electron microscopy (SEM), and N_2 adsorption-desorption. SEM was carried out on a Hitachi (model S-4160) apparatus after gold plating of the samples. XRD patterns were recorded with a Bruker D8-Advance diffractometer at 2θ = 2°–70° with monochromatized K_α radiation (λ = 0.1541874 nm) from a Cu source operated at 40 kV/30 mA. FT-IR spectra were obtained with an EQUINOX 55BRUKER. N_2 adsorption-desorption isotherms were obtained using a BELSORP-mini II at −196 °C. All samples were degassed at 100 °C for 3 h under an inert gas flow before measurement. The BET equation was used to calculate specific surface area and the BJH equation was used to calculate the pore size distribution and total pore volume.

1.3 Synthesis of catalysts

1.3.1 Synthesis of g-C_3N_4 and Fe-g-C_3N_4

g-C_3N_4 was prepared using the method reported by Wang et al. [18]. In a typical reaction, dicyandiamide (1 g) was mixed with distilled water (10 ml) and heated to remove the solvent. The resulting mixture was heated at 600 °C for 4 h under flowing argon, followed by cooling to room temperature under the inert atmosphere. For the synthesis of Fe-g-C_3N_4, different amounts of $FeCl_3{\cdot}6H_2O$ (0.1, 0.2, 0.3 g) were added to the mixture of dicyandiamide (1 g) and distilled water (10 ml), and then this solution was heated until a dry product was obtained. Different amounts of $FeCl_3$ were loaded on g-C_3N_4 to obtain *x*Fe-g-C_3N_4 (*x* = 10%, 20%, 30%).

1.3.2 Synthesis of *x*Fe-g-C_3N_4-LUS-1

In a typical synthesis, LUS-1 (1 g, prepared using the method reported by Badiei et al. [37]) was dispersed in distilled water (30 ml) with vigorous stirring (named mixture A). An amount of $FeCl_3{\cdot}6H_2O$ and dicyandiamide were dissolved in distilled water (30 ml) (iron(III) chloride/dicyandiamide = 0.1), which was named solution B. Solution B was gradually added to mixture A to prepare *x*Fe-g-C_3N_4-LUS-1 (*x* (wt%) = [dicyandiamide/LUS-1] × 100%). The mixture of solution A and solution B was heated at 100 °C to remove water until a reddish mixture was obtained. Finally, the product was obtained by heating the reddish material at 600 °C under an inert atmosphere for 4 h.

1.3.3 Catalytic test

Catalytic experiments were done to investigate the activity of the catalysts for the conversion of benzene to phenol. Solvent (4 ml acetonitrile) was poured into a 50 ml round bottom flask equipped with a condenser and the temperature was raised to 60 °C. Benzene (1 ml, 11.3 mmol) and well milled catalyst (50 mg) were added to the flask. After 0.5 h stirring, hydrogen peroxide (H_2O_2 30 wt%, 0.5 ml, 16.5 mmol) was added to the mixture and the reaction mixture was stirred for 4 h. Then, 5 ml ethanol was poured into the flask to stop the reaction by capturing remaining hydroxyl radicals (OH·) and convert the biphasic mixture into a single phase [38]. All reactions were carried out in dark and in sunlight (the sunlight reactions were done on sunny days with an intensity of about 80000 LUX) to evaluate the effect of light on the catalytic activity of g-C_3N_4. In addition, the photocatalytic activities of these catalysts were investigated using an artificial visible light source (125 W mercury lamp with an intensity about 67000 LUX with colored filter). The quantitative analysis of the product was done with a Perkin-Elmer 8500 GC with an FID detector and toluene as the internal standard.

2 Result and discussion

2.1 XRD results

Wide angle XRD patterns were used to characterize the structures of Fe-g-C_3N_4, LUS-1, and Fe-g-C_3N_4-LUS-1. The results are shown in Fig. 1. The predicted structure of g-C_3N_4 based on tri-*s*-triazine building blocks (Franklin's model) would exhibit two major diffraction peaks in the XRD pattern corresponding to the (100) and (002) reflection planes [20,26,33]. Here, these peaks were observed in the XRD patterns of the synthesized materials (Fig. 1). This result proved that the synthesized g-C_3N_4 structure was that predicted by Franklin's model [21,39]. As shown in Fig. 1(3), two peaks at 13.3° and 27.4° were seen, which were

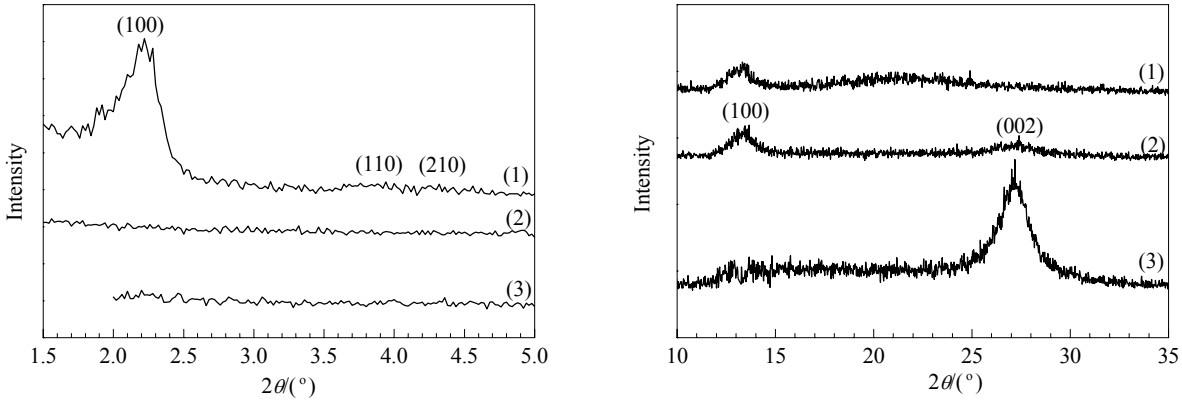

Fig. 1. XRD patterns of Fe-g-C_3N_4-LUS-1 (1), Fe-g-C_3N_4 (2), and g-C_3N_4 (3).

related to the hole-to-hole and interlayer distance of g-C_3N_4, respectively. The first peak was attributed to the in-plane structural packing of the carbon nitride layers. The peaks at 13.3° and 27.4° gave d_{100} = 0.665 nm and d_{002} = 0.326 nm, respectively [33]. The XRD pattern of Fe-g-C_3N_4 (Fig. 1(2)) showed similar peaks with a small shift and a significant decrease in the intensity for the latter peak (27.4° to 27.2°). This observed shift in diffraction angle revealed that d_{002} was increased to 0.328 nm. In the case of the less intense 27.2° diffraction, it was concluded that the introducing of the iron species into the g-C_3N_4 structure was successful, and this caused lower crystallinity and consequently lower diffraction intensity. From the increase in d_{002} and decrease in 27.2° peak intensity, it can be proposed that the iron species were loaded between the graphitic layers of carbon nitrides. With increasing Fe loading in g-C_3N_4, the crystallinity of Fe-g-C_3N_4 decreased. Our results were in good agreement with those of other research groups [40].

The XRD pattern of Fe-g-C_3N_4-LUS-1 is shown in Fig 1(1). This pattern showed the structural peaks of LUS-1 [34], which confirmed that the LUS-1 structure was retained. The comparison between the XRD patterns of g-C_3N_4 and Fe-g-C_3N_4-LUS-1 revealed the disappearance of the peak at 27.4°, but no change in the intensity of the other peak at 13.3°. With Fe-g-C_3N_4, the (002) peak was not detected due to its very low intensity. In addition to other possibilities for the disappearance of the peak at 27.4°, another interesting structure can be suggested: it is a single layer of g-C_3N_4 formed in the pores of LUS-1. The complete understanding of this structure needs more studies.

2.2 FT-IR results

The FT-IR spectra of the samples are shown in Fig. 2. Figure 2(3)–(6) showed a strong absorption peak at 800 cm^{-1}, which was attributed to the characteristic breathing mode of the triazine ring [33,41]. Usually, absorption peaks

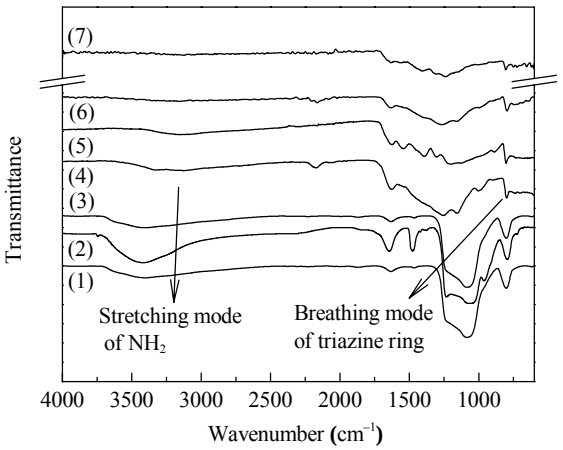

Fig. 2. FT-IR spectra of LUS-1 (1), 20%Fe-g-C_3N_4-LUS-1 (2), 10%Fe-g-C_3N_4-LUS-1 (3), g-C_3N_4 (4), 10%Fe-g-C_3N_4 (5), 20%Fe-g-C_3N_4 (6), and 30%Fe-g-C_3N_4 (7).

due to the stretching mode of C–N, C=N, ring stretching and N–H bending vibration in the heterocyclic aromatic ring system are observed as bands in the 1000–1700 cm^{-1} region [23,24,31]. The FT-IR spectra of g-C_3N_4 and Fe-g-C_3N_4 showed these peaks. In the case of *x*Fe-g-C_3N_4-LUS-1 (*x* = 10% and 20%), compounds containing C–N and C=N bonds were incorporated into the structure of the silica support LUS-1 (Fig. 2(1)) and the overlap of the strong broad peaks of Si–O–Si with these peaks makes it impossible to assign the C–N and C=N peaks in Fe-g-C_3N_4-LUS-1. In addition, the C≡N stretching vibration was observed as a weak absorption peak appearing at 2200 cm^{-1} and the bands at 3000–3300 cm^{-1} can be assigned to the stretching mode of NH and NH_2.

2.3 N_2 adsorption-desorption results

The nitrogen adsorption-desorption isotherms for LUS-1 and Fe-g-C_3N_4-LUS-1 are shown in Fig. 3. The LUS-1 material showed a Type IV isotherm that showed the presence

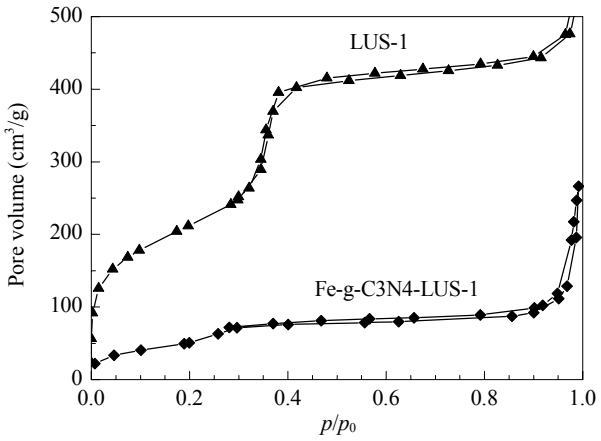

Fig. 3. N_2 adsorption-desorption isotherms of LUS-1 and 10%Fe-g-C_3N_4-LUS-1.

of mesopores in this material (Fig. 3). On the other hand, the adsorption-desorption isotherm of Fe-g-C_3N_4-LUS-1 was a deformed Type IV (Fig. 3) isotherm. It can be concluded that the introduction of Fe-g-C_3N_4 into LUS-1 caused the surface area, average pore diameter, and pore volume of Fe-g-C_3N_4-LUS-1 to be lower than those of LUS-1. From the data in Table 1, due to the loading of the graphitic carbon nitride in the pores of LUS-1, its surface area was decreased. In 30%Fe-g-C_3N_4-LUS-1, the pores of LUS-1 were blocked and the surface area was much decreased to 25 m^2/g. Therefore, 30%Fe-g-C_3N_4-LUS-1 was not used in the reaction experiments. The structural parameters of these materials are shown in Table 1.

2.4 SEM results

SEM images of LUS-1 and Fe-g-C_3N_4-LUS-1 are shown in Fig. 4. These SEM images gave the morphology of LUS-1 before and after Fe-g-C_3N_4 loading. As the morphology of the Fe-g-C_3N_4-LUS-1 did not change during the reaction, it can be proposed that the morphology of the mesoporous silica was stable under the reaction conditions.

Table 1 Specific surface area, pore radius, and total pore volume of LUS-1 and *x*Fe-g-C_3N_4-LUS-1

Sample	A_{BET}/ (m^2/g)	Pore radius (nm)	Total pore volume (cm^3/g)
LUS-1	776	1.64	0.84
Fe-g-C_3N_4	10	—	—
10%Fe-g-C_3N_4-LUS-1	194	1.21	0.35
20%Fe-g-C_3N_4-LUS-1	149.3	1.21	0.31
30%Fe-g-C_3N_4-LUS-1	25	—	—

2.5 Catalytic activity

The catalytic reaction results are shown in Fig. 5, Fig. 6, Table 2, and Table 3. The effects of various factors including the amount of H_2O_2, light source, and iron content on the hydroxylation of benzene to phenol were investigated.

2.5.1 Effect of light source

All reactions were done under both dark and sunlight conditions to investigate the effect of light on the reaction performance. From Table 2, the phenol yields in the dark were negligible compared with those in light. The catalytic performance was remarkably enhanced when the reaction condition was changed to be in sunlight. It can be suggested that g-C_3N_4 adsorbed sunlight and activated Fenton's reagent. In addition, the decomposition of H_2O_2 increased in the presence of sunlight and this produced more hydroxyl radicals. Hydroxyl radicals attack the benzene molecules and produce phenol and other hydroxylated species. To study the effect of an artificial light source on the reaction performance, a Hg lamp with a colored filter (violet filter) was used as a visible light source. The results of these experiments are also shown in Table 2. When the added hydrogen peroxide was 0.5 ml, the phenol yields of 10%Fe-g-C_3N_4 were 5% and 5.6% for visible light and sunlight reactions, respectively. This observation indicated that the photocatalytic activity of these materials was ap-

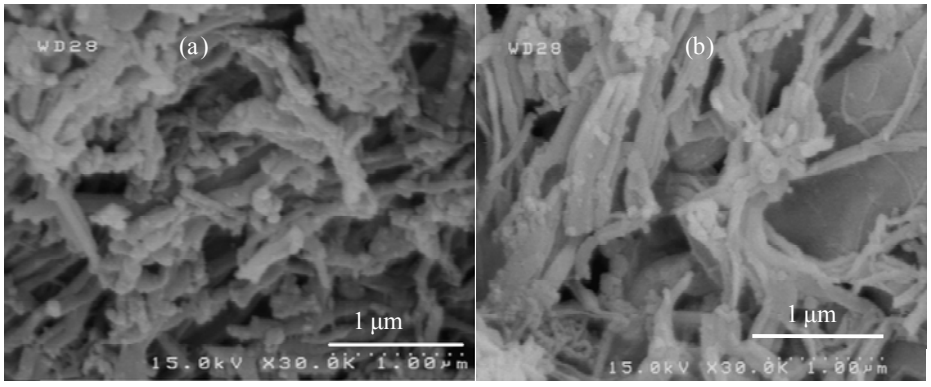

Fig. 4. SEM images of LUS-1 (a) and 10%Fe-g-C_3N_4-LUS-1 (b).

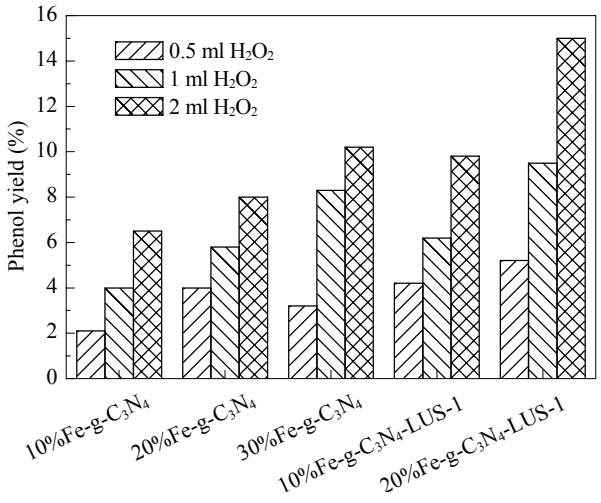

Fig. 5. Catalytic activity of g-C_3N_4 based catalysts in the hydroxylation of benzene under sunlight in the presence of different amounts of H_2O_2. Reaction conditions: 1 ml benzene, 4 ml acetonitrile, 0.05 g catalyst, reaction temperature 60 °C. Phenol yield was calculated according to the moles of produced phenol/moles of initial benzene.

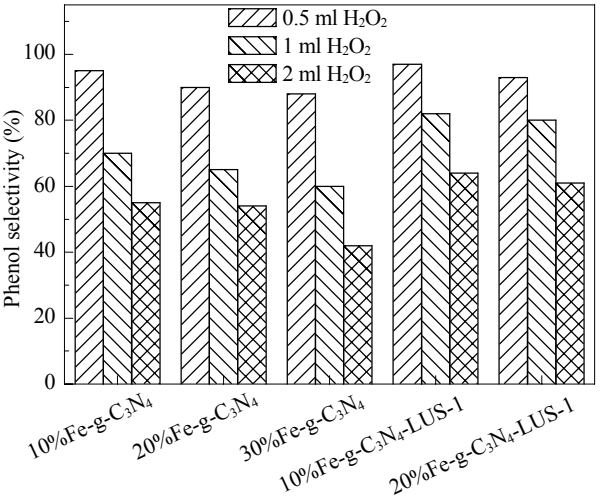

Fig. 6. Phenol selectivity of the catalysts in the presence of different amounts of H_2O_2 under sunlight. Reaction condition: 1 ml benzene, 4 ml acetonitrile, 0.05 g catalyst, reaction temperature 60 °C. Phenol selectivity was calculated according to the moles of produced phenol/moles of reacted benzene.

proximately similar for the two conditions. Thus, it can be suggested that the effect of the 125 W Hg lamp and sunlight on the hydroxylation of benzene was similar. Therefore, all reactions were done in sunlight instead of the expensive artificial visible light source.

Table 3 TOF of the catalysts in the presence of different amounts of hydrogen peroxide under sunlight

Sample	TOF (10^2 h^{-1})		
	0.5 ml	1 ml	2 ml
10%Fe-g-C_3N_4	23.7	45.2	73.4
20%Fe-g-C_3N_4	49.1	71.2	98.3
30%Fe-g-C_3N_4	67.2	112	137.2
10%Fe-g-C_3N_4-LUS-1	674	942	1570
20%Fe-g-C_3N_4-LUS-1	479	856	1370

2.5.2 Effect of H_2O_2

When the amount of hydrogen peroxide was increased from 0.5 to 2 ml, the phenol yield increased from 2.1% to 6.5% for 10%Fe-g-C_3N_4, 4% to 8% for 20%Fe-g-C_3N_4, and 5% to 10.2% for 30%Fe-g-C_3N_4. The increase in phenol yield in the presence of more hydrogen peroxide was attributed to the increase of hydroxyl radicals in the reaction mixture, which attack benzene rings and produce more hydroxylated species of benzene. However, the use of more hydrogen peroxide resulted in less phenol selectivity. Side reactions occurred when hydroxyl radicals were added, and these produced other hydroxylated species of benzene such as catechol, benzoquinone, etc.

2.5.3 Effect of iron content

To evaluate the effect of iron loading on the hydroxylation of benzene, graphitic carbon nitride (g-C_3N_4) with different amounts of iron content was synthesized. When the iron content was increased, the phenol yield was enhanced. For example, when the added hydrogen peroxide was 2 ml, the phenol yield was increased from 6.5% to 10.5% for 10%Fe-g-C_3N_4 and 30%Fe-g-C_3N_4, respectively. This observation and the mechanism (Fenton's reaction) of benzene hydroxylation were useful for interpreting the effect of iron content on the hydroxylation reaction. Briefly, the presence of more active iron species in the reaction mixture gave more of the necessary hydroxyl radicals. Thus, more benzene molecules were converted to the hydroxylated form.

2.5.4 Comparison of unsupported and supported catalysts

The effect of using a support on the reaction was investi-

Table 2 Phenol yield (%) of Fe-g-C_3N_4 under sunlight and visible light conditions in the presence of different amount of H_2O_2

Sample	0.5 ml H_2O_2			2 ml H_2O_2		
	Dark	Sunlight	Visible light	Dark	Sunlight	Visible light
10%Fe-g-C_3N_4–LUS-1	0.8	4.3	4	2.1	10	9.8
20%Fe-g-C_3N_4-LUS-1	1.8	5.6	5	4.7	16	15.6

The phenol yield was calculated according to produced phenol/initial benzene.

gated. The results are shown in Figs. 5 and 6. For this comparison, mesoporous LUS-1 was used as a porous support and different amounts of *x*Fe-g-C_3N_4 were incorporated into it (*x* = 10%, 20%). When the amount of added hydrogen peroxide was 2 ml, the phenol yield was increased from 8% to 16% by loading 20%Fe-g-C_3N_4 on the surface of LUS-1. This result showed that the catalytic activity of graphitic carbon nitride was remarkably enhanced by using a support. In addition, it can be seen in Fig. 6 that on adding more H_2O_2, the selectivity for phenol decreased with both supported and unsupported catalysts. However, a smaller decrease in phenol selectivity was observed when the supported catalyst was used. From these results, it can be suggested that LUS-1 stabilized the phenol produced and protected it from more oxidation.

2.5.5 Investigation of TOF

The effects of various parameters on the turnover frequency (TOF) in the hydroxylation of benzene are shown in Table 3. The TOF was defined as moles of produced phenol per melem unit per hour. The TOF was increased by adding hydrogen peroxide into the reaction mixtures. In addition, with unsupported catalysts, the TOF was enhanced by increasing the iron loading. With these catalysts, increasing iron loading gave increased phenol yield at approximately a constant amount of melem units. However, with the supported catalysts, by increasing the amount of g-C_3N_4 in LUS-1, the TOF was decreased. In these reactions, the enhancing of produced phenols was negligible with increasing melem units.

3 Conclusions

g-C_3N_4, *x*-Fe-g-C_3N_4 and *x*-Fe-g-C_3N_4-LUS-1 were prepared and characterized by XRD, FT-IR, N_2 adsorption. and SEM. Their catalytic activity for the hydroxylation of benzene was investigated. The catalytic activity of Fe-g-C_3N_4 was remarkably increased from dark to sunlight reaction conditions. The phenol yield increased on increasing either the amount of hydrogen peroxide or iron loading. The phenol selectivity was increased by loading Fe-g-C_3N_4 in LUS-1. g-C_3N_4 can be used as a photocatalyst in sunlight and does not need an expensive artificial light source.

References

1 Pan J H, Dou H, Xiong Z, Xu C, Ma J, Zhao X S. *J Mater Chem*, 2010, **20**: 451
2 Wang J, Li R, Zhang Z, Sun W, Xu R, Xie Y, Xing Z, Zhang X. *Appl Catal A*, 2008, **334**: 227
3 Goettmann F, Fischer A, Antonietti M, Thomas A. *New J Chem*, 2007, **31**: 1455
4 Pan H, Li X, Zhuang Z, Zhang C. *J Mol Catal A*, 2011, **345**: 90
5 Sun J H, Dong S Y, Feng J L, Yin X J, Zhao X C. *J Mol Catal A*, 2011, **335**: 145
6 Li K, Martin D, Tang J. *Chin J Catal*, 2011, **32**: 879
7 Oh W-C, Chen M, Cho K, Kim C, Meng Z, Zhu L. *Chin J Catal*, 2011, **32**: 1577
8 Xiao Y, Dang L, An L, Bai S, Lei Z. *Chin J Catal*, 2008, **29**: 31
9 Ao Y, Xu J, Zhang S, Fu D. *J Phys Chem Solids*, 2009, **70**: 1042
10 Guan G, Kida T, Yoshida A. *Appl Catal B*, 2003, **41**: 387
11 Kuai L, Geng B, Chen X, Zhao Y, Luo Y. *Langmuir*, 2010, **26**: 18723
12 Vidya K, Kamble V S, Selvam P, Gupta N M. *Appl Catal B*, 2004, **54**: 145
13 Hou L-R, Yuan C-Z, Peng Y. *J Mol Catal A*, 2006, **252**: 132
14 Nezamzadeh-Ejhieh A, Hushmandrad S. *Appl Catal A*, 2010, **388**: 149
15 Sonawane R S, Dongare M K. *J Mol Catal A*, 2006, **243**: 68
16 Wang Z-Y, Chou H-C, Wu J C S, Tsai D P, Mul G. *Appl Catal A*, 2010, **380**: 172
17 Ke D, Peng T, Ma L, Cai P, Jiang P. *Appl Catal A*, 2008, **350**: 111
18 Chen X, Zhang J, Fu X, Antonietti M, Wang X. *J Am Chem Soc*, 2009, **131**: 11658
19 Zhang J, Chen X, Takanabe K, Maeda K, Domen K, Epping J D, Fu X, Antonieta M, Wang X. *Angew Chem, Int Ed*, 2010, **49**: 441
20 Thomas A, Fischer A, Goettmann F, Antonietti M, Müller J O, Schlögl R, Carlsson J M. *J Mater Chem*, 2008, **18**: 4893
21 Komatsu T. *J Mater Chem*, 2001, **11**: 799
22 Komatsu T. *Macromol Chem Phys*, 2001, **202**: 19
23 Zhang Z, Leinenweber K, Bauer M, Garvie L A J, McMillan P F, Wolf G H. *J Am Chem Soc*, 2001, **123**: 7788
24 Guo Q, Xie Y, Wang X, Lv S, Hou T, Liu X. *Chem Phys Lett*, 2003, **380**: 84
25 Montigaud H, Tanguy B, Demazeau G, Alves I, Courjault S. *J Mater Sci*, 2000, **35**: 2547
26 Lotsch B V, Schnick W. *Chem Mater*, 2006, **18**: 1891
27 Bojdys M J, Müller J O, Antonietti M, Thomas A. *Chem Eur J*, 2008, **14**: 8177
28 Montigaud H, Tanguy B, Demazeau G, Alves I, Birot M, Dunogues J. *Diamond Relat Mater*, 1999, **8**: 1707
29 Bai Y J, Lü B, Liu Z G, Li L, Cui D L, Xu X G, Wang Q L. *J Cryst Growth*, 2003, **247**: 505
30 Zhao H, Chen X L, Jia C, Zhou T, Qu X, Jian J, Xu Y. *Mater Sci Eng B*, 2005, **122**: 226
31 Li X, Zhang J, Shen L, Ma Y, Lei W, Cui Q, Zou G. *Appl Phys A*, 2009, **94**: 387
32 Yan S C, Li Z S, Zou Z G. *Langmuir*, 2010, **26**: 3894
33 Yan S C, Li Z S, Zou Z G. *Langmuir*, 2009, **25**: 10397
34 Gholami J, Badiei A, Abbasi A, Ziarani G M. *Int J ChemTech Res*, 2009, **1**: 426

35 Martínez F, Calleja G, Melero J A, Molina R. *Appl Catal B*, 2005, **60**: 181
36 Sirotin S V, Moskovskaya I F. *Petrol Chem*, 2009, **49**: 99
37 Badiei A, Bonneviot L, Crowther N, Mohammadi Ziarani G. *J Organomet Chem*, 2006, **691**: 5911
38 Arab P, Badiei A, Koolivand A, Mohammadi Ziarani G. *Chin J Catal*, 2011, **32**: 258
39 Franklin E C. *J Am Chem Soc*, 1922, **44**: 486
40 Wang X, Chen X, Thomas A, Fu X, Antonietti M. *Adv Mater*, 2009, **21**: 1609
41 Guo Q, Xie Y, Wang X, Zhang S, Hou T, Lv S. *Chem Commun*, 2004: 26

《催化学报》2011 年 SCI 影响因子首次突破 1.0

根据美国汤森路透 (Thomson Reuters) 2012 年 6 月 29 日公布的 2011 年度《期刊引证报告》 (*Journal Citation Reports*, *JCR*),《催化学报》2011 年 SCI 影响因子首次突破 1.0, 达到 1.171, 总被引频次为 1529, 5 年影响因子为 0.945. 其中, 影响因子和 5 年影响因子均位居 SCI 收录的中文化学类期刊第 1 名, 也是历年来我国中文化学类期刊 SCI 影响因子的最高值. 这表明,《催化学报》正在被越来越多的国内外同行阅读和参考, 该刊在国际学术交流中的作用进一步提高. 《催化学报》取得的成绩离不开广大作者、审稿专家和读者多年来的大力支持和帮助, 在此向您表示衷心感谢!

(《催化学报》编辑部 2012-07-02)

2011 Impact Factor of *Chinese Journal of Catalysis* is 1.171

According to the 2011 *Journal Citation Reports* (*JCR*) published by Thomson Reuters, the impact factor of *Chinese Journal of Catalysis* reached 1.171, which is 56% higher than the previous year. This has been the highest SCI impact factor of *Chinese Journal of Catalysis* since she was included in the Science Citation Index-Expanded (SCI-E) in 2001, indicating that the Journal is now read and referred by more and more readers in the world.

(Editorial Office of *Chinese Journal of Catalysis*, 2012-07-02)